

# NUMERICAL ESTIMATION OF LOSSES IN STEAM FLOW THROUGH LP TURBINE BLADE ROWS

SŁAWOMIR DYKAS AND WŁODZIMIERZ WRÓBLEWSKI

*Institute of Power Engineering and Turbomachinery,  
Silesian University of Technology,  
Konarskiego 18, PL 44100 Gliwice, Poland  
dykas@rie5.ise.polsl.gliwice.pl*

(Received 13 March 2006)

**Abstract:** The aim of this work is to estimate the losses in steam flow through an LP steam turbine rotor and the whole stage. Two types of losses occur in steam flow, aerodynamic (profile, secondary flow, leakage) and thermodynamic (due to addition of heat caused by condensation). The presented numerical results are split into two groups. First, a comparison of three different calculation methods of steam flow is carried out. To this end, the geometry of an LP steam turbine's last rotor is chosen. The first examined method is the Streamline Curvature Method (SCM) used on the meridional plane with loss correlations, the other two being commercial and in-house CFD codes, solving the Reynolds-averaged Navier-Stokes equations for a 3D flow. The first two codes model equilibrium steam properties below the saturation line, while the latter models non-equilibrium steam properties. Finally, a comparison is made of the influence on loss prediction of various condensation models for the geometry of the penultimate stage, with the use of an in-house CFD code.

**Keywords:** LP steam turbine, wet steam, condensation, losses

## Nomenclature

$N$  – power [W]  
 $h$  – specific enthalpy [J/kg]  
 $p$  – pressure [Pa]  
 $R$  – individual gas constant [J/kg K]  
 $s$  – specific entropy [J/(kg K)]  
 $T$  – temperature [K]  
 $v$  – velocity [m/s]  
 $y$  – non-equilibrium wetness fraction [kg/kg]  
 $z$  – compressibility coefficient  
 $\rho$  – density [kg/m<sup>3</sup>]  
 $\Delta$  – quantity increase

### Subscripts

1 – inlet  
2 – outlet

$c$  – condenser  
 $g$  – vapor phase  
 $l$  – liquid phase  
 $s$  – isentropic quantity

#### Abbreviations

LP – Low-Pressure  
SCM – Streamline Curvature Method

## 1. Introduction

Ever more reliable methods and algorithms of through-flow optimization are devised thanks to the development of CFD numerical methods and accumulation of knowledge on energy dissipation in thermal fluid-flow machinery flows. Together with increased computer efficiency they enable us to abandon the simplifications of numerical flow modeling and consider real geometries of steam turbines.

The losses in the last stages of LP steam turbines are difficult to estimate. This is mainly due to a significant parameter change along the blade length, transonic and supersonic flows and the two-phase character of the flow. Two types of losses have to be considered in the last stages: aerodynamic losses due to the interaction between the fluid and the wall boundaries and thermodynamic losses occurring during the phase change.

Loss prediction for fluid-flow machinery has attracted the interest of many researchers. There has been both experimental (*e.g.* [1–3]) and numerical research [4, 5] in this field. In the method based on a numerical solution of flow-governing equations, the losses in steam turbines are in most cases calculated with the use of an ideal gas model. It is a justified simplification when the stages operate on superheated steam. However, there problems may arise with proper calculation of the entropy increase or enthalpy drop. For LP stages operating on the wet steam, an ideal gas equation of state cannot be used as a mathematical closure of flow-governing equations, as an estimation of entropy production would be incorrect. At the same time, the application of a real gas equation of state creates many additional problems in the numerical algorithm for the solution of flow-governing equations [6]. Calculations become more time-consuming due to the additional iteration processes necessary for steam parameter estimation and boundary condition algorithms.

In the first part of this paper, losses are estimated on the basis of flow parameters determined by means of three different algorithms. The first one is based on the Streamline Curvature Method. The calculation results depend on the assumed relations describing the energy losses. The progress in numerical modeling has made it possible to determine the 3D flow structure more accurately. The other algorithms used in the calculations are based on the finite volume method. The TASCflow commercial codes and TraCoFlow, an in-house CFD code have been used. The TraCoFlow code is able to account for thermodynamic losses caused by condensation (the non-equilibrium model), whereas the TASCflow code uses the equilibrium dry/wet steam model. Numerical investigations have been performed on the geometry of the LP part of a high-output steam turbine.

In the second part of the paper, the TraCoFlow CFD code is used to investigate the influence of different condensation models on the losses. The flow without

condensation, with homogeneous condensation and with heterogeneous condensation is modeled. The geometry of an LP steam turbine's penultimate stage has been chosen for these calculations.

## 2. Numerical analysis

Accurate determination of the flow field parameters is required for a correct estimate of losses in steam flow through the turbine stage. The flow field can be predicted by means of various physical and numerical methods. Three numerical methods are applied in this paper: the 2D Streamline Curvature Method, the TASCflow commercial CFD code and TraCoFlow, an in-house code.

### 2.1. The Streamline Curvature Method (SCM)

The classical Streamline Curvature Method is used to simulate the flow in the meridional plane. In this method, a real gas equation of state for water steam is applied [7]. Empirical formulas are used for energy dissipation in the conservation equations. The losses are divided into profile, boundary and additional ones, including leakage losses. The empirical correlations proposed by Craig and Cox [8] are used save for long blades, where the relations given by Aleksejeva [9] are implemented.

### 2.2. TASCflow (commercial CFD code)

TASCflow v.2.11.1 [10] is a code widely used for turbomachinery applications. TASCflow is based on the averaged Navier-Stokes equations employing the finite volume method (FVM) with an implicit, multi-block algorithm. The solution strategy is based on the algebraic multi-grid method. TASCflow provides many types of turbulence models. In this case, turbulence is modeled with the use of Menter's SST (Shear-Stress-Transport) model [11, 12]. In TASCflow, the real gas flow is modeled using an approximation of water steam tables. The equilibrium model for a two-phase flow has been assumed in the presented calculations.

### 2.3. TraCoFlow (in-house CFD code)

The third method for predicting the flow field is an in-house CFD code. The numerical simulation is based on time-dependent, 3D Reynolds-averaged Navier-Stokes equations coupled with a two-equation turbulence model (the  $k$ - $\omega$  SST model), with additional mass-conservation equations for the liquid phase (two for homogeneous condensation and one for heterogeneous condensation). The set of governing equations is closed by a 'local' real-gas equation of state [6]. The application of a real gas equation of state as a mathematical closure of partial-differential equations complicates the numerical algorithm significantly. The idea behind the use of a real gas equation of state has been to create a very accurate equation as simple in mathematical form as possible. As the flow through turbine stages takes place within a limited range of steam parameters, an equation of state covering the whole region of superheated steam is not necessary. A simple mathematical form can be very accurate only in a small parameter range. Therefore, a new form of the equation of state for real gases has been created (Figure 1).

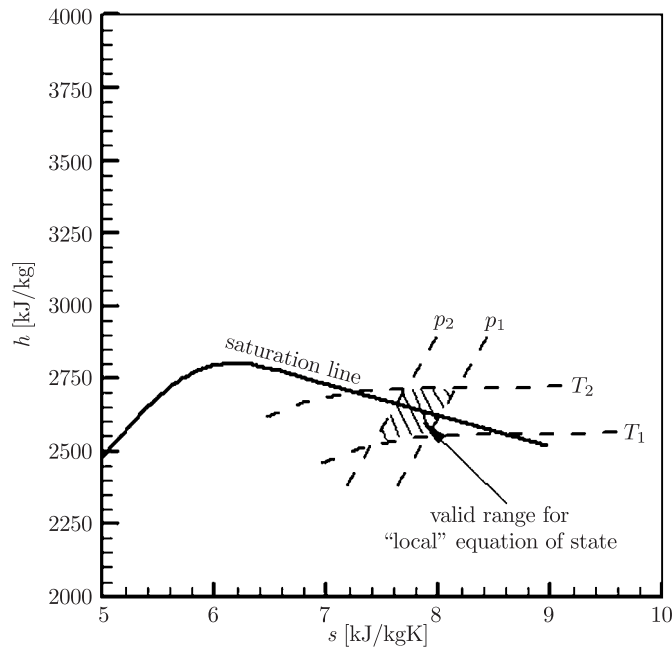


**Figure 1.** Mollier's diagram of the "local" real gas equation of state near the saturation line

The mathematical form of the applied real-gas equation of state, Equation (1), is similar to the virial equation of state with a single virial coefficient:

$$\frac{p}{\rho \cdot R \cdot T} = z(T, \rho) = A(T) + B(T) \cdot \rho, \quad (1)$$

where

$$\begin{aligned} A(T) &= a_0 + a_1 \cdot T + a_2 \cdot T^2, \\ B(T) &= b_0 + b_1 \cdot T + b_2 \cdot T^2. \end{aligned}$$

Coefficients  $a_i$ ,  $b_i$  ( $i = 0 \dots 2$ ) of polynomials  $A(T)$  and  $B(T)$  are functions of temperature only and can be found from an approximation of the thermodynamic properties of steam IAPWS-IF'97 [13]. The equation is represented with a relatively uncomplicated approximate surface (see Figure 2).

Equation (1) is called the 'local' real-gas equation of state, as – because of its simple mathematical form – it can be applied locally in a limited parameter range.

This form of the 'local' real-gas equation of state can be applied to various arbitrary real gases, including steam. For modeling the ideal gas flow, it is enough to assume that  $a_0 = 1$  and  $a_1, a_2, b_0, b_1, b_2 = 0$ .

For two-phase flow, it is assumed that the volume occupied by droplets is negligibly small. The droplets formed by homogeneous nucleation are very small and growing. The interaction between the droplets has been neglected in the model, as has been Heat exchange between the liquid phase and the solid boundary, and the velocity slip between the vapor and the liquid phase. The non-slip assumption is much less significant than the effects of thermal non-equilibrium [14]. On this assumption, the momentum conservation equations may have the same form as for single-phase flow.

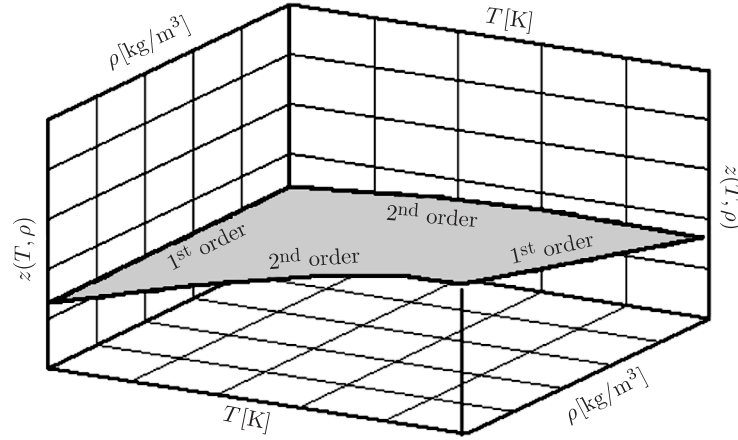


Figure 2. Approximate surface of the IAPWS-IF97 properties

The conservation equations have been formulated for the two-phase mixture with the specific parameters calculated with the following relations:

$$h = h_g(1-y) + h_1y, \quad s = s_g(1-y) + s_1y, \quad \rho = \rho_g/(1-y). \quad (2)$$

The value of the non-equilibrium wetness fraction,  $y$ , has been calculated from the conservation equations for the liquid phase.

The condensation phenomena have been modeled on the basis of the classical nucleation theory of Volmer, Frenkel and Zeldovich, well-suited for modeling technical flows [15, 16]. In this theory, the rate of formation of droplet embryos per mass unit of mixture,  $J$  (the nucleation rate), the droplet growth rate,  $dr/dt$ , and the critical droplet radius,  $r^*$ , have to be modeled. The nucleation rate,  $J$ , is calculated with the correction factor proposed by Kantrowitz [17]. The equation of droplet growth for steam flow requires a relation valid for a wide range of Knudsen numbers. Therefore, the continuous model proposed by Gyarmathy [18] is used in the presented method.

For heterogeneous condensation on insoluble particles, an additional equation has to be solved for the liquid phase. The model of heterogeneous condensation on soluble particles is based on [19].

The system of governing equations is solved on a multi-block structured grid with the finite volume method and integrated in time with the explicit Runge-Kutta method. In time integration, the fractional step method is used to split the equations into homogeneous and inhomogeneous parts in order to introduce various time steps for the flow and condensation calculations.

The MUSCL technique has been implemented to approach the TVD scheme with the flux limiter to avoid oscillations. A detailed description of the method can be found in Wróblewski [20] and Dykas [6].

#### 2.4. Loss coefficient

There are many loss coefficients used in loss estimation for cascade flow. The basic correlation uses increase in entropy and is known as the cascade (or entropy) loss coefficient:

$$\zeta = \frac{T_2 \Delta s}{\frac{1}{2} v_2^2} = \frac{T_2 \Delta s}{\Delta h_s + \frac{1}{2} v_1^2}. \quad (3)$$

In the case of flow through rotors, relative velocities are used in Equation (3), absolute velocities have to be used for stators. For 3D test cases the coefficient is calculated along the blade's length from circumferentially mass-averaged values. In the Streamline Curvature Method, the parameters are treated as circumferentially averaged.

### 3. Calculation results

A numerical analysis was carried out for the geometry of the last stage rotor and for the penultimate stage of a 200MW LP steam turbine. Boundary conditions at the inlet and outlet for the TASCflow and TraCoFlow CFD codes were determined from results obtained with the Streamline Curvature Method, which assured the same boundary conditions for all the performed calculations. The Streamline Curvature Method was used for calculations of the flow through the whole LP part of the steam turbine. It made it possible, with known inlet and outlet conditions for the LP part, to determine the radial parameter distributions in the gaps between blade rows and to locate condensation.

Exactly the same numerical grid was applied for the TASCflow and TraCoFlow CFD codes. The calculation results represent the steady flow field, which means that the presented losses are time-averaged. A mixed-out technique was used model the stator-rotor interaction. In the last stages of the LP steam turbine the flow has a strong 3D character and the stream line is difficult to identify. Therefore, the losses were calculated using mass-averaged flow parameters at the inlet and outlet.

A very important parameter of the turbine flow is the power generated through the stage. Therefore, beside the cascade loss coefficient, stage power was used as an additional parameter for comparison. It was calculated for the TraCoFlow results only.

Stage power was calculated with two methods. In one method, the resultant moment was determined from static pressure distribution on the rotor blade surface. With rotation speed and a known number of blades, power could be calculated. The advantage of this method is that it is enough to model the flow through the rotor to estimate the whole stage power. In the other method, power was calculated with the use of enthalpy drop in the stage and the mass flow rate. The power calculated with both methods should have the same value. In the case of the TraCoFlow CFD code, the difference between these two methods of power estimation was less than 0.5%.

#### 3.1. LP steam turbine's last rotor

The rotor geometry of the LP steam turbine's last stage was chosen for comparison of the different methods of flow field prediction (Figure 3). The gap between the rotor's tip and the casing was not modeled and thus leakage losses were neglected. Two different operating conditions were considered for the last stage, relatively far from the nominal load. They correspond to the power of  $N = 140\text{MW}$  by two values of pressure in the condenser ( $p_c = 2.7\text{kPa}$  and  $p_c = 3.7\text{kPa}$ ), as under these conditions condensation starts in the last stage. The radial distributions of inlet angles and total parameters at the rotor's inlet were determined for both cases by means of SCM.

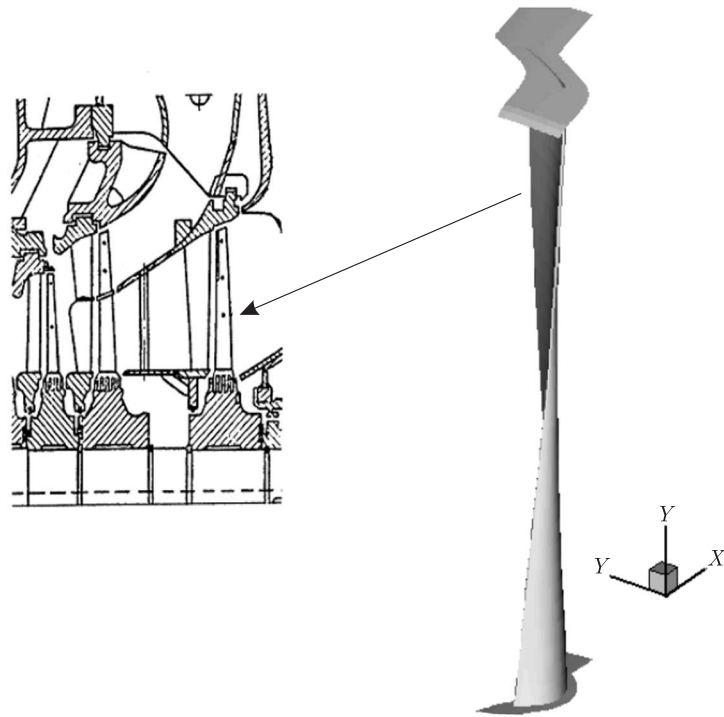


**Figure 3.** Geometry for an LP steam turbine's last stage rotor

The computational domain was discretized with a structural multi-block grid. The dimensionless distance of the first grid line from solid walls,  $y^+$ , was less than 1.5. Numerical grid for the last rotor consisted of about 260 000 nodes. The Reynolds number calculated with the total parameters at the inlet, the inlet speed of sound and the blade chord was  $Re = 0.17 \cdot 10^6$ .

Our earlier research has demonstrated that for the methods used here the number of grid points close to 250 000 for one blade row makes the solution grid independent. A further increase in the number of grid points does not alter the flow field significantly and or change the values of the loss coefficient (for steady flow without tip leakage).

A comparison of the loss coefficient's distributions calculated using different methods of flow field prediction is shown in Figure 4. In this case, the loss coefficient distributions along the blade span are relatively close to each other. There is relatively good agreement between the SCM and TraCoFlow calculations with the adiabatic flow model (without condensation), which is attributable to wetness losses not being modeled in SCM. In both cases, the greatest losses were incurred for the flow with homogeneous condensation modeled by the TraCoFlow code.

TASCflow models an equilibrium wet steam flow and the loss coefficient distribution calculated on the basis of its results is lower than for the flow with condensation and higher than for the adiabatic flow.

In the case with higher pressure in the condenser, the outlet wetness is higher than in the case with lower outlet pressure, as expansion proceeds with lower values of entropy.

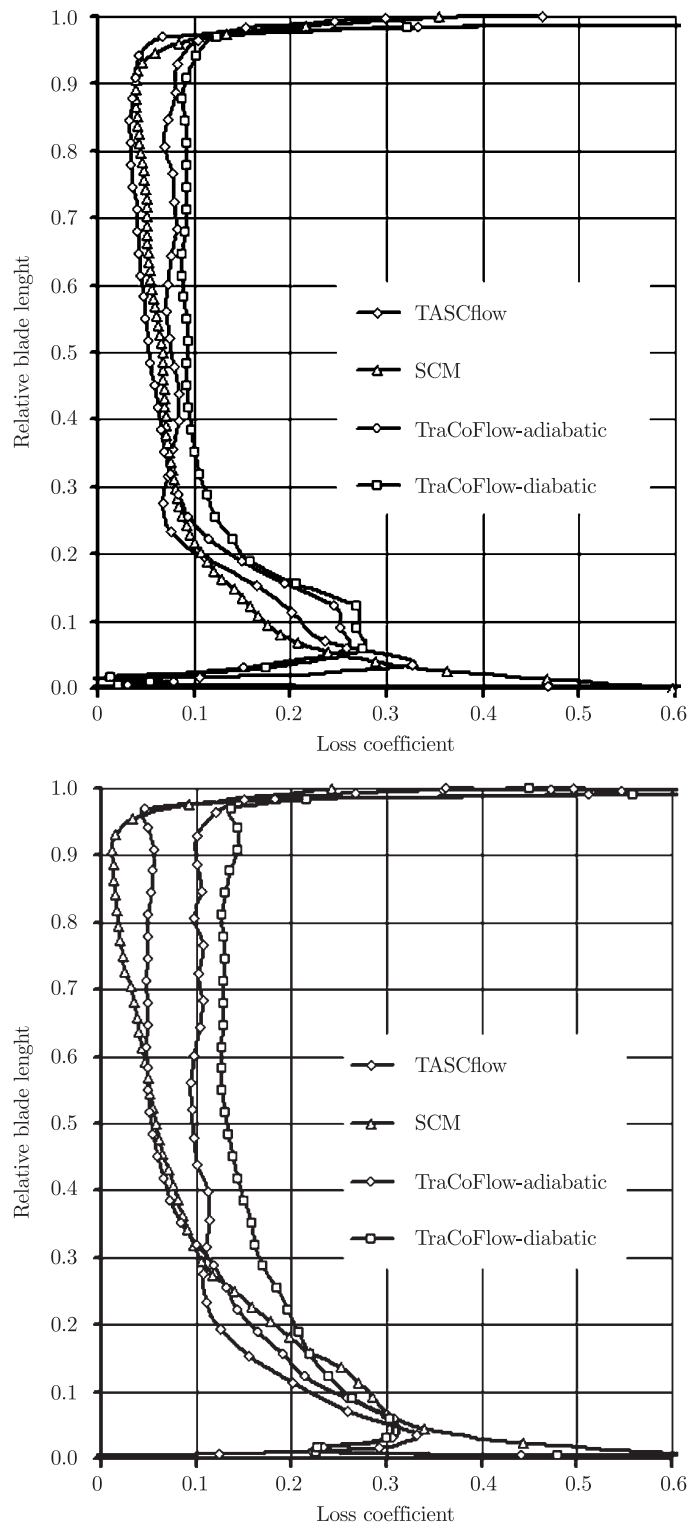
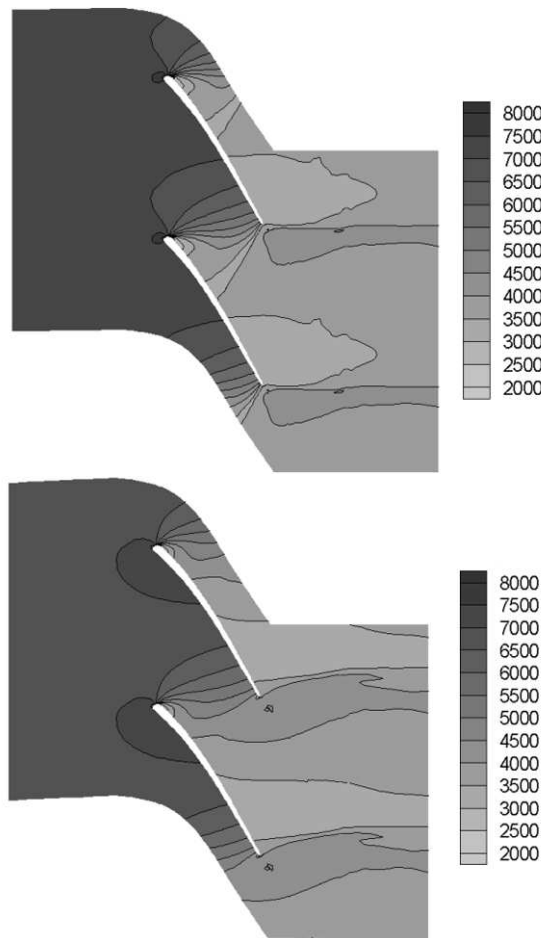


Figure 4. Comparison of the loss coefficient for last stage rotor



**Table 1.** Values of stage power calculated with the TraCoFlow CFD code

	adiabatic	homogeneous condensation
power [MW]	2.95	3.05
$N = 140\text{MW}, p_c = 3.7\text{kPa}$		
power [MW]	3.12	3.07
$N = 140\text{MW}, p_c = 2.7\text{kPa}$		



**Figure 5.** Pressure distribution  $P$  [Pa] at the tip section for the last stage rotor for  $N = 140\text{MW}$  and  $p_c = 3.7\text{kPa}$  (TraCoFlow results)

Additionally, the power generated through the last stage rotor was determined with the TraCoFlow code. Table 1 shows a comparison of power for the flow with and without homogeneous condensation.

Apparently, in some cases condensation may increase the power slightly in comparison with the adiabatic flow, in spite of the losses caused by the condensing flow being higher (Figure 4). This may be due to the change of the shock wave moving from the trailing edge to the suction side of the blade (Figure 5). The weakness of this shock wave causes a decrease in the pressure on the suction side, which may affect

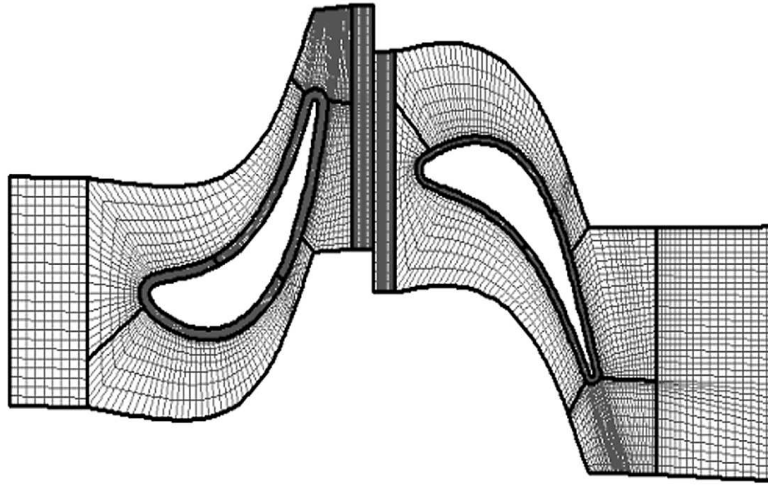


**Figure 6.** Numerical grid at mid-span for stage calculation ( $\sim 240\,000$  nodes for each blade row)

power. Besides, we consider that the entropy loss coefficient, Equation (3), depends not only on  $\Delta s$  but also on the outlet temperature and velocity. Usually, the outlet temperature for diabatic flow is higher than for adiabatic one. In effect, with an insignificant difference in  $\Delta s$  between diabatic and adiabatic flows, the loss coefficient for diabatic flow can be much greater than for adiabatic one.

### 3.2. LP steam turbine's penultimate stage

It is clear, *e.g.* from the former calculations, that the flow model has a significant influence on the value of losses in a wet steam flow. The TraCoFlow code has been chosen to investigate various wet steam models, as only this code enables one to calculate the wet steam flow with different condensation models. In TASCflow v.2.11.1, the homogeneous condensation model (NES) is implemented too, but we were unable to obtain satisfactory results with this code, even for a 2D cascade flow and with the help of CFX experts.

For this comparison, the geometry of the penultimate stage of another large-output steam turbine was selected. The number of nodes for each blade row was about 240 000, with  $y^+$  of less than 1.5 (Figure 6). The total parameters at the inlet were  $p_0 = 52\,000\text{Pa}$ ,  $T_0 = 373.15\text{K}$ , while the outlet static pressure was  $p_{out} = 22\,000\text{Pa}$ . The Reynolds number for this flow case was  $\text{Re} = 1.1 \cdot 10^6$ .

Four types of flow were applied for comparison: flow without condensation (adiabatic flow), flow with homogeneous condensation, and flow with heterogeneous condensation on insoluble and soluble particles (NaCl). A concentration of  $10^{15}$  particles per cubic meter and the radius of  $10^{-8}$  meter were assumed for heterogeneous condensation.

The obtained span-wise distributions of the loss coefficient are presented in Figure 7. The loss coefficient for the stator, Equation (3), was calculated with absolute velocities. As in the previous cases, relative velocities were used for the rotor. An increase of the loss coefficient for diabatic flow with heterogeneous condensation has been observed for the stator. It is connected with the appearance of the liquid phase at

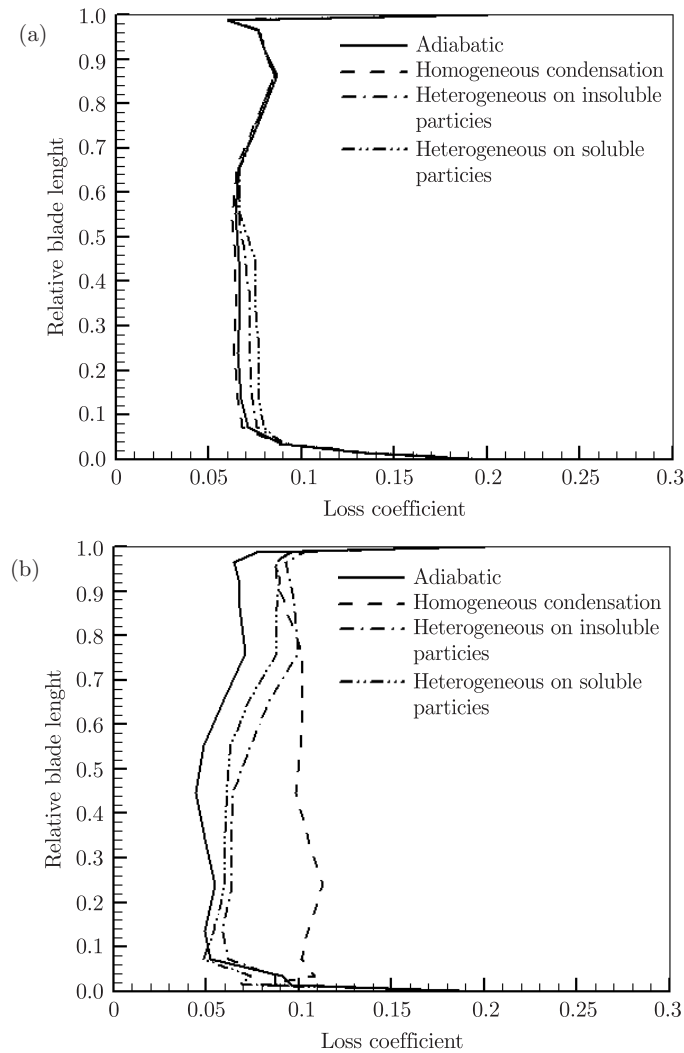


**Figure 7.** Span-wise distribution of the loss coefficient for the penultimate stage: (a) stator, (b) rotor

the stator’s outlet (see Figure 8). In the rotor, heterogeneous condensation produces lower losses than homogeneous one, as in the case of homogeneous condensation a rapid increase of pressure and entropy is observed.

Figure 8 shows the static temperature and wetness fraction distributions in the blade-to-blade channels at the mid-span of the stage blades. The outlet value of the wetness fraction is very similar for all types of condensation and equals  $\sim 3.5\%$ . For the flow with homogeneous condensation, the wetness fraction has been observed only in the rotor (homogeneous condensation starts, as usual, close to the transition from sub- to supersonic flow – the Mach number close to 1). Heterogeneous condensation shifts the wetness fraction upstream towards the stator. In the case of condensation on soluble particles, formation of the wetness fraction starts just above the saturation line.

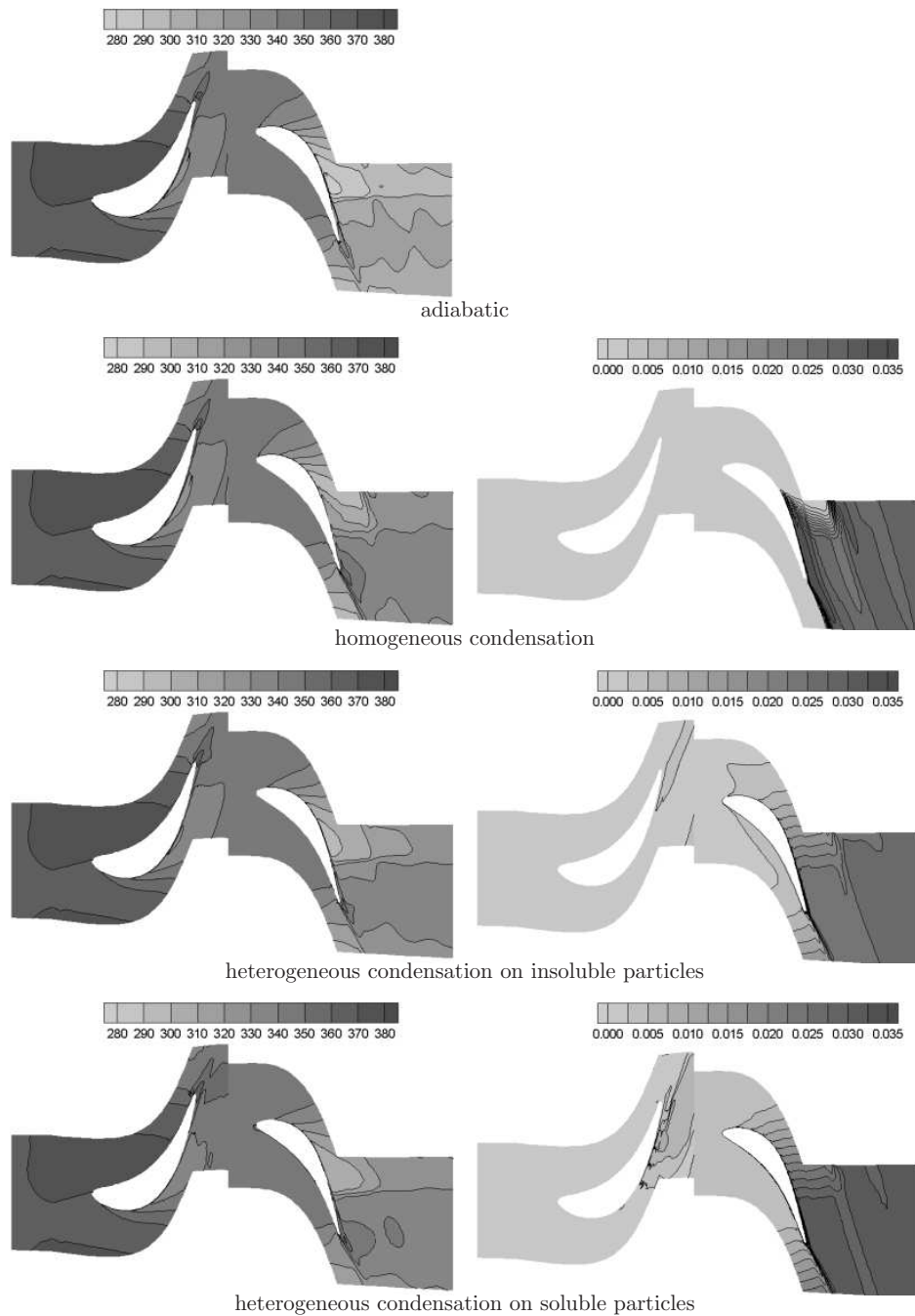


**Figure 8.** Parameter distribution in the stage at mid-span:  
static temperature  $T$  [K] (left) and wetness fraction  $Y_{\text{hom}} + Y_{\text{het}}$  [kg/kg] (right)

The calculated power for the penultimate stage and the mass flow for all four flow models are presented in Table 2.

The higher power and mass flow have been observed for the flow without condensation. The drop in power and mass flow in comparison to the adiabatic flow is

**Table 2.** Values of stage power and mass flow calculated with the TraCoFlow CFD code

	adiabatic	homogeneous condensation	heterogeneous condensation on insoluble particles	heterogeneous condensation on soluble particles
power [MW]	7.41	7.33	7.34	7.32
mass flow [kg/s]	63.25	62.75	62.58	62.4

similar for all condensing flows, which suggests that the condensation model does not influence the change of power and mass flow significantly. The value of the outlet wetness fraction is similar in all cases, only the location of condensation is different. It is known from earlier calculations [6] that flows with mixed homogeneous/heterogeneous condensation have the strongest effect on the losses and power. In the presented heterogeneous flow on insoluble and soluble particles, condensation is almost purely heterogeneous.

### 4. Conclusions

Three methods of fluid flow calculation are used to estimate the loss coefficient in the last stage rotor. The presented methods use different dry/wet steam models. The finite volume calculation methods, TASCflow and TraCoFlow, are compared with the Streamline Curvature Method with empirical correlations for loss coefficients. The elaborated in-house CFD code allows calculating a steam-condensing flow in LP steam turbine stages for a wide range of operating parameters.

An analysis of losses in a flow without condensation, with homogeneous and heterogeneous condensation, has been carried out. The influence of impurities' concentration on the losses has also been investigated. The in-house code has been used for condensing flows. A comparison of results obtained with TraCoFlow and TASCflow has shown:

- good correspondence between the flow field parameters for the flow without condensation,
- good correspondence in the modeling of steam (real gas) properties. (The simplest equation of state used in the in-house code has given results identical to those of the virial equation of state with three virial coefficients applied in TASCflow.)

Qualitatively, all three methods have given similar loss coefficient distributions. The differences have resulted from the different flow models assumed in the calculations.

The Streamline Curvature Method is suitable to determine the inlet and outlet boundary conditions for TASCflow and TraCoFlow 3D calculations. Radial parameters distributions in blade row gaps can be obtained from calculations for the whole LP part.

The following conclusions can be drawn for a 3D flow through the penultimate stage of an LP steam turbine:

- for the flow with heterogeneous condensation wetness appears earlier,
- the solubility of particles may alter the location of condensation in the turbine stage,

- the flow with homogeneous condensation is the worst with respect to efficiency and losses, and
- the influence of impurities on the flow field is significant, but it is very difficult to determine the distribution, size, type and impurities' concentration in a real turbine.

Thermodynamic losses have to be taken into account in order to estimate losses in a wet steam flow correctly. It is impossible to calculate these types of flows properly with the adiabatic model (especially with an ideal gas equation of state).

### References

- [1] Bohn D and Holzenthal K 1997 *Proc. 2<sup>nd</sup> European Conf. on Turbomachinery*, Antwerpen, Belgium, pp. 55–63
- [2] Dibelius G H, Mertens K, Pitt R U and Strauf E 1987 *Proc. Inst. of Mech. Eng., Conf. on Turbomachinery-Efficiency, Prediction and Improvement*, Cambridge, UK, pp. 135–143
- [3] Vomela J 2002 *Power Machines 2002, Conf. WBU, Pilsen* (no pagination)
- [4] Bohn D, Surken N and Kreitmeier F 2003 *Proc. 5<sup>th</sup> European Conf. on Turbomachinery*, Prague, pp. 741–751
- [5] Lampart P 2003 *Proc. 5<sup>th</sup> European Conf. on Turbomachinery*, Prague, pp. 771–783
- [6] Dykas S 2001 *TASK Quart.* **5** (4) 519
- [7] Chmielniak T and Łukowicz H 1995 *Flow Investigations for Different Loads of Blade Cascade*, ZN Politechniki Śląskiej, No. 126, Gliwice (in Polish)
- [8] Craig H R M and Cox H J A 1970–1971 *J. of the Inst. of Mech. Eng.* **32** 407
- [9] Aleksejeva R N and Bojcová E A 1973 *Teploenergetika* **12** 21 (in Russian)
- [10] *CFX-TASCflow, Theory Documentation* 2001, Version 2.11, AEA Technology, Canada
- [11] Menter F R 1994 *AIAA J.* **32** 1598
- [12] Menter F R 1996 *J. Fluids Eng.* **118** 514
- [13] Wagner W *et al.* 2000 *J. of Engng Gas Turbines and Power* **122** 150
- [14] White A J, Young J B and Walters P T 1996 *Phil. Trans. R. Soc. Lond. A.* 354
- [15] Frenkel J 1955 *Kinetic Theory of Liquids*, Dover Publ., New York
- [16] Fuchs N A and Satugin A G 1971 *High-Dispersed Aerosols, Topics in Current Aerosols Research* (Hidy G M and Brock J R, Eds.), Pergamon Press, London
- [17] Kantrowitz A 1951 *J. Chem. Phys.* **19** 1097
- [18] Gyarmathy G 1960 *Grundlagen einer Theorie der Nassdampfturbine*, Dissertation, Juris Verlag, Zürich
- [19] Gorbunov B and Hamilton R 1997 *J. Aerosol Sci.* **28** (2) 239
- [20] Wróblewski W 2000 *Numerical Simulation of the Flow Phenomena in Thermal Turbines*, ZN Politechniki Śląskiej, Energetyka, No. 132 (in Polish)